

Cardiff University
School of Physics and Astronomy

Doctor of Philosophy Thesis

The Silicon Cold Electron Bolometer

by

Thomas Leonard Robert Brien

June 2014

Supervisors: Professor Philip D. Mauskopf
Professor Peter A. R. Ade
Doctor Gao Min
Doctor Simon M. Doyle
Doctor Dan E. Read

To ...

Acknowledgements

Firstly I'd like to thank the academy.

Contents

Acknowledgments	i
Contents	iii
1 Chapter's title	1
1.1 Introduction	1
2 Chapter's title	5
3 Detector Readout	7
3.1 Introduction	7
3.2 Requirements of the Readout System	8
3.3 Initial Testing System	8
3.3.1 Initial Readout System	8
3.3.2 Initial Bias System	14
3.4 Revisions to the Initial Bias System	18
3.4.1 Changes Made and Advantages	18
3.4.2 Performance of Updated Bias System	21
3.5 Final Testing System	23
3.5.1 Reason for replacement	23
3.5.2 Final Readout System	24
3.5.3 Final Bias System	30
3.6 Cross-Correlated Noise Measurement	34
3.6.1 Convolution & Cross-Correlation	34
Acronyms	37

Glossary	39
A Appendix title	45
List of Figures	47
List of Tables	48
Index	49

Chapter One

Chapter's title

*“Begin at the beginning,” the King said gravely, “and
go on till you come to the end: then stop.”*
— Lewis Carroll, *Alice in Wonderland*

1.1 INTRODUCTION

... some text ...

Lorem ipsum dolor sit amet, consectetur adipiscing elit. Ut purus elit, vestibulum ut, placerat ac, adipiscing vitae, felis. Curabitur dictum gravida mauris. Nam arcu libero, nonummy eget, consectetur id, vulputate a, magna. Donec vehicula augue eu neque. Pellentesque habitant morbi tristique senectus et netus et malesuada fames ac turpis egestas. Mauris ut leo. Cras viverra metus rhoncus sem. Nulla et lectus vestibulum urna fringilla ultrices. Phasellus eu tellus sit amet tortor gravida placerat. Integer sapien est, iaculis in, pretium quis, viverra ac, nunc. Praesent eget sem vel leo ultrices bibendum. Aenean faucibus. Morbi dolor nulla, malesuada eu, pulvinar at, mollis ac, nulla. Curabitur auctor semper nulla. Donec varius orci eget risus. Duis nibh mi, congue eu, accumsan eleifend, sagittis quis, diam. Duis eget orci sit amet orci dignissim rutrum.

Nam dui ligula, fringilla a, euismod sodales, sollicitudin vel, wisi. Morbi auctor lorem non justo. Nam lacus libero, pretium at, lobortis vitae, ultricies et, tellus. Donec aliquet, tortor sed accumsan bibendum, erat ligula aliquet magna, vitae

ornare odio metus a mi. Morbi ac orci et nisl hendrerit mollis. Suspendisse ut massa. Cras nec ante. Pellentesque a nulla. Cum sociis natoque penatibus et magnis dis parturient montes, nascetur ridiculus mus. Aliquam tincidunt urna. Nulla ullamcorper vestibulum turpis. Pellentesque cursus luctus mauris.

Nulla malesuada porttitor diam. Donec felis erat, congue non, volutpat at, tincidunt tristique, libero. Vivamus viverra fermentum felis. Donec nonummy pellentesque ante. Phasellus adipiscing semper elit. Proin fermentum massa ac quam. Sed diam turpis, molestie vitae, placerat a, molestie nec, leo. Maecenas lacinia. Nam ipsum ligula, eleifend at, accumsan nec, suscipit a, ipsum. Morbi blandit ligula feugiat magna. Nunc eleifend consequat lorem. Sed lacinia nulla vitae enim. Pellentesque tincidunt purus vel magna. Integer non enim. Praesent euismod nunc eu purus. Donec bibendum quam in tellus. Nullam cursus pulvinar lectus. Donec et mi. Nam vulputate metus eu enim. Vestibulum pellentesque felis eu massa.

Quisque ullamcorper placerat ipsum. Cras nibh. Morbi vel justo vitae lacus tincidunt ultrices. Lorem ipsum dolor sit amet, consectetur adipiscing elit. In hac habitasse platea dictumst. Integer tempus convallis augue. Etiam facilisis. Nunc elementum fermentum wisi. Aenean placerat. Ut imperdiet, enim sed gravida sollicitudin, felis odio placerat quam, ac pulvinar elit purus eget enim. Nunc vitae tortor. Proin tempus nibh sit amet nisl. Vivamus quis tortor vitae risus porta vehicula.

Fusce mauris. Vestibulum luctus nibh at lectus. Sed bibendum, nulla a faucibus semper, leo velit ultricies tellus, ac venenatis arcu wisi vel nisl. Vestibulum diam. Aliquam pellentesque, augue quis sagittis posuere, turpis lacus congue quam, in hendrerit risus eros eget felis. Maecenas eget erat in sapien mattis porttitor. Vestibulum porttitor. Nulla facilisi. Sed a turpis eu lacus commodo facilisis. Morbi fringilla, wisi in dignissim interdum, justo lectus sagittis dui, et vehicula libero dui cursus dui. Mauris tempor ligula sed lacus. Duis cursus enim ut augue. Cras ac magna. Cras nulla. Nulla egestas. Curabitur a leo. Quisque egestas wisi eget nunc. Nam feugiat lacus vel est. Curabitur consectetur.

Suspendisse vel felis. Ut lorem lorem, interdum eu, tincidunt sit amet, laoreet vitae, arcu. Aenean faucibus pede eu ante. Praesent enim elit, rutrum at, molestie non, nonummy vel, nisl. Ut lectus eros, malesuada sit amet, fermentum eu, sodales cursus, magna. Donec eu purus. Quisque vehicula, urna sed ultricies

auctor, pede lorem egestas dui, et convallis elit erat sed nulla. Donec luctus. Curabitur et nunc. Aliquam dolor odio, commodo pretium, ultricies non, pharetra in, velit. Integer arcu est, nonummy in, fermentum faucibus, egestas vel, odio.

Sed commodo posuere pede. Mauris ut est. Ut quis purus. Sed ac odio. Sed vehicula hendrerit sem. Duis non odio. Morbi ut dui. Sed accumsan risus eget odio. In hac habitasse platea dictumst. Pellentesque non elit. Fusce sed justo eu urna porta tincidunt. Mauris felis odio, sollicitudin sed, volutpat a, ornare ac, erat. Morbi quis dolor. Donec pellentesque, erat ac sagittis semper, nunc dui lobortis purus, quis congue purus metus ultricies tellus. Proin et quam. Class aptent taciti sociosqu ad litora torquent per conubia nostra, per inceptos hymenaeos. Praesent sapien turpis, fermentum vel, eleifend faucibus, vehicula eu, lacus.

Pellentesque habitant morbi tristique senectus et netus et malesuada fames ac turpis egestas. Donec odio elit, dictum in, hendrerit sit amet, egestas sed, leo. Praesent feugiat sapien aliquet odio. Integer vitae justo. Aliquam vestibulum fringilla lorem. Sed neque lectus, consectetur at, consectetur sed, eleifend ac, lectus. Nulla facilisi. Pellentesque eget lectus. Proin eu metus. Sed porttitor. In hac habitasse platea dictumst. Suspendisse eu lectus. Ut mi mi, lacinia sit amet, placerat et, mollis vitae, dui. Sed ante tellus, tristique ut, iaculis eu, malesuada ac, dui. Mauris nibh leo, facilisis non, adipiscing quis, ultrices a, dui.

Morbi luctus, wisi viverra faucibus pretium, nibh est placerat odio, nec commodo wisi enim eget quam. Quisque libero justo, consectetur a, feugiat vitae, porttitor eu, libero. Suspendisse sed mauris vitae elit sollicitudin malesuada. Maecenas ultricies eros sit amet ante. Ut venenatis velit. Maecenas sed mi eget dui varius euismod. Phasellus aliquet volutpat odio. Vestibulum ante ipsum primis in faucibus orci luctus et ultrices posuere cubilia Curae; Pellentesque sit amet pede ac sem eleifend consectetur. Nullam elementum, urna vel imperdiet sodales, elit ipsum pharetra ligula, ac pretium ante justo a nulla. Curabitur tristique arcu eu metus. Vestibulum lectus. Proin mauris. Proin eu nunc eu urna hendrerit faucibus. Aliquam auctor, pede consequat laoreet varius, eros tellus scelerisque quam, pellentesque hendrerit ipsum dolor sed augue. Nulla nec lacus.

Suspendisse vitae elit. Aliquam arcu neque, ornare in, ullamcorper quis, commodo eu, libero. Fusce sagittis erat at erat tristique mollis. Maecenas sapien libero, molestie et, lobortis in, sodales eget, dui. Morbi ultrices rutrum lorem. Nam elementum ullamcorper leo. Morbi dui. Aliquam sagittis. Nunc placerat.

Pellentesque tristique sodales est. Maecenas imperdiet lacinia velit. Cras non urna. Morbi eros pede, suscipit ac, varius vel, egestas non, eros. Praesent malesuada, diam id pretium elementum, eros sem dictum tortor, vel consectetur odio sem sed wisi.

Chapter Two

Chapter's title

... some text ...

Some reference **Led2004**

Some symbols: DMC, LZ77, LZ78.

Chapter Three

Detector Readout

“The audience is the most revered member of the theater. Without an audience there is no theater.”
— Viola Spolin

3.1 INTRODUCTION

Like all high-sensitivity detectors operating in the far-infrared (**Rieke2007**), cold electrons bolometers need to be readout using amplification. Amplification is of either the voltage or the current, with the quantity not being amplified for readout usually providing the bias. **Golubev2001** provide a good discussion of the advantages and disadvantages of current-bias versus voltage-bias for use with Cold Electron Bolometers (CEBs), along with a basic schematic for each case.

In reality the Superconducting Quantum Interference Devices (SQUIDs) and their associated electronics used to amplify current in a voltage bias regime are both more expensive and more complex to setup compared to the voltage amplifiers used for current biased measurements. This means that it is often preferable to use a current biased system for early device development.

During the development of Silicon Cold Electron Bolometers (SiCEBs) numerous iterations of voltage amplifier have been used. Each readout system was designed to offer the possibility of improved device characterisation, from either a

lower contribution to the noise measurement or by allowing measuring to higher frequencies of readout.

In addition to changes that were required to the amplification system is has also been necessary to change the exact technique by which the detector has been biased. The main driver for these changes has been the desire to reduce electrical noise input to the device as well as to create the most stable and capable testing regime possible.

3.2 REQUIREMENTS OF THE READOUT SYSTEM

In order to specify a readout system it is important to define a number of desirable goals for its performance. For the early development stage testing of CEBs the following desired points were set:

- The system had to be as simple as possible. This is to say that the design and operation of the readout should not become a distraction from the testing of devices.
- The system needed contribute a sufficiently low electrical noise that noise measurements of the detector could be successfully performed.
- The system was capable of measuring the speed of response of the detector by measurement of the roll-off of device noise.

Although it was possible to estimate both the speed and expected noise levels for a CEB, these estimates were only vague ‘ball-park’ figures. This meant that it was necessary to produce an testing system believed to be capable of meeting these criteria and then to make improvements as required. Further to these requirements any system needed to be able to perform DC-measurements, such as recording current-voltage (IV) curves with a high degree of stability.

3.3 INITIAL TESTING SYSTEM

3.3.1 INITIAL READOUT SYSTEM

The initial amplification system used was heavily based upon an existing circuit designed to readout Resistance Temperature Detectors (RTDs). This was used as

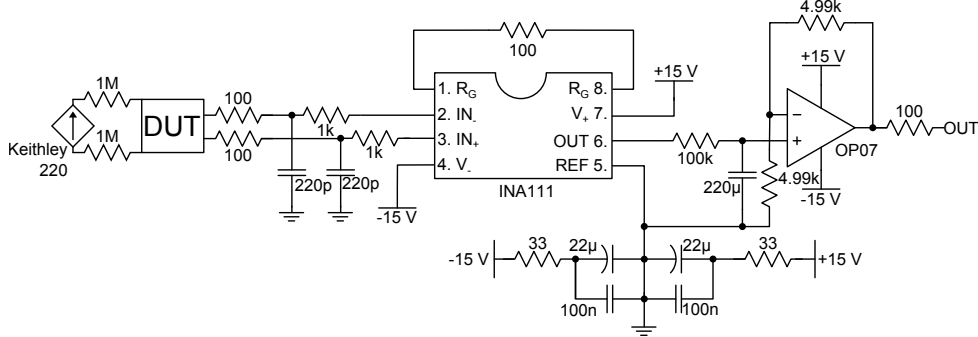


Figure 3.1: Initial bias and readout system using a Keithley 220 programmable current source to bias the device under test (DUT). The voltage is then amplified by the INA111 differential amplifier (configured for a gain factor of 500) and then by the OP07 operational-amplifier (configured to give a gain of two).

it was readily available within the department and early (somewhat optimistic) estimations of device performance indicated that noise measurements would be possible. This amplifier was used in conjuncture with a Keithly 220 Programmable Current Source to provide the bias across the device. Figure 3.1 shows the circuit diagram of the amplifier used here along with the connection of current source. To perform an IV measurement the current source, which is controlled by a computer, is stepped through the desired range of values and at each step a data acquisition unit (DAQ) records the amplified voltage across the device.

The **INA1112010** and **OP07DS** state that both these amplifiers have, when operating in the configuration shown in Figure 3.1, a noise voltage, referred to the input, of $10 \text{ nVHz}^{-1/2}$. In order to understand how the internal noise of these amplifiers contributes to the total noise measured at the output of the system we can think of each of the two amplifiers as containing some source which generates a noise voltage with a spectral density of e_n and some *black-box* which provides the gain while generating no noise. This is illustrated in Figure 3.2.

In Figure 3.2 we see that if there is no input signal at point I then the input to the second amplifier, point A, will consist of only the noise generated in the first amplifier, multiplied by that amplifier's gain factor. The, uncorrelated, noise from the second amplifier is then added to the amplified noise from the first and both are multiplied by the gain of the second amplifier. From this we can define the

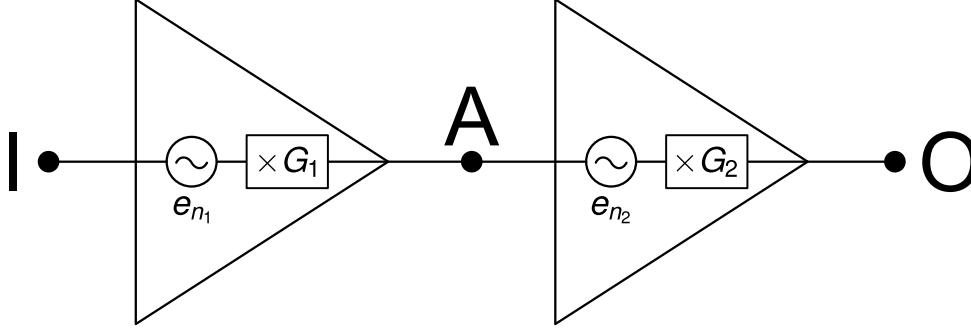


Figure 3.2: Simple model of two amplifiers working in series. Each amplifier contains a component which generates a noise voltage with spectral density e_n before an ideal, noiseless, component amplifies the signal by a gain factor of G .

total noise, e_{tot} , at the output of this system, in the absence of any input signal, as:

$$e_{tot} = \sqrt{(e_{n1} \times G_1)^2 + e_{n2}^2 \times G_2}. \quad (3.1)$$

If, as is the case in Figure 3.1, $e_{n1} \times G_1 \gg e_{n2}$ then we can say:

$$e_{tot} \approx e_{n1} G_1 G_2. \quad (3.2)$$

We can define the input referred noise voltage spectral density, e_{RTI} , simply as:

$$e_{RTI} = \frac{e_{tot}}{G_{tot}}, \quad (3.3)$$

where G_{tot} is the product of the various gain stages, given by:

$$G_{tot} = \prod_n G_n. \quad (3.4)$$

By applying Equation 3.1 for the system shown in Figure 3.1 ($e_{n1} = e_{n2} = 10 \text{ nVHz}^{-1/2}$, $G_1 = 500$ and $G_2 = 2$) we find that $e_{RTI} = 10.00002 \text{ nVHz}^{-1/2}$. The above approximation can be verified by calculating e_{RTI} again using Equation 3.2, this gives $e_{RTI} \approx 10 \text{ nVHz}^{-1/2}$. This shows that in this case the internal noise from the second amplifier is contributing only 0.0002 % of the noise at the output.

It is possible to characterise the amplifier by measuring three simple parameters, the amplifier's: gain, bandwidth and internal noise. The gain can be found

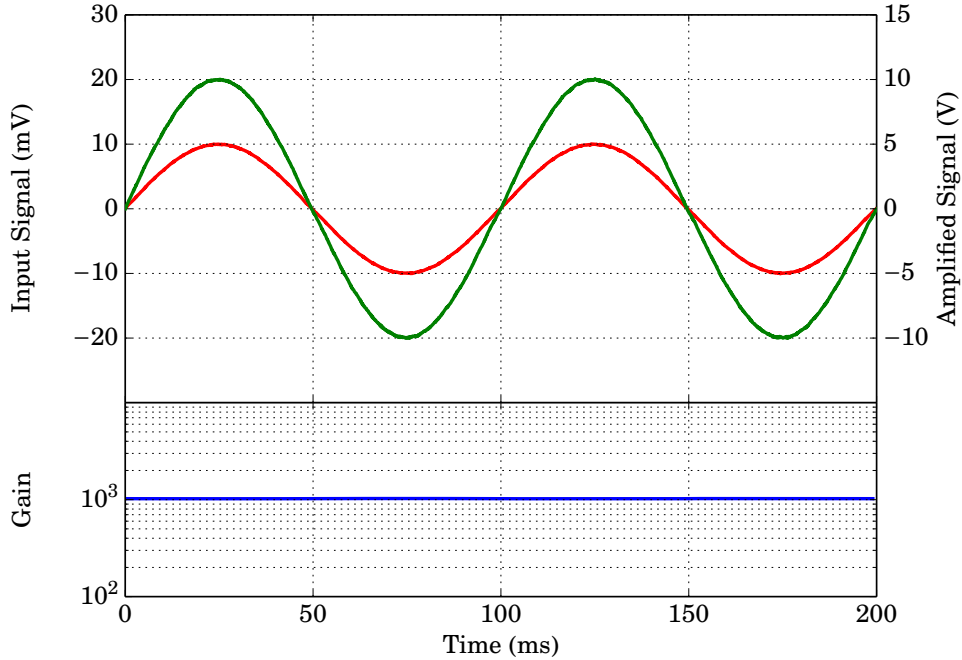


Figure 3.3: Gain measurement of RTD amplifier using a 10 Hz sinusoidal wave. Upper plot – Input signal (red, primary vertical axis) compared to the amplified signal (green, secondary vertical axis). Lower plot – Gain measured from taking the ratio of the amplified and input signals.

by measuring how much a signal, a simple sinusoidal wave for example, is amplified; the bandwidth of the amplifier can be found by measuring the frequency at which the noise spectral density decreases from $e_{tot}G_{tot}$ (this can also serve as a measure of the uniformity of the gain across a wide range of frequencies). Finally the internal noise (referred to the amplifiers input) can be found from the noise spectral density, corrected for the measured gain, when the input of the amplifier is shorted (no input signal).

Figure 3.3 shows the amplification of a 10 Hz sinusoidal wave generated by a signal generator, the output of which was split between the amplifier to be tested and a direct input to a digital oscilloscope. The input signal (red, shown on the primary vertical axis of the upper plot of Figure 3.3) was measured to have a peak amplitude of 10 mV ($V_{rms} = 7.07$ mV). The amplified signal (green, secondary

vertical scale) was measured as having a peak amplitude of 10 V ($V_{rms} = 7.07$ V), from this it is clear the gain factor of the amplifier is 1000 at the voltage peaks. The uniformity of the gain, for various input amplitudes, was verified by simply taking the ratio of these two signal at all points, the result of this is shown in the lower plot of Figure 3.3, from this it is clear that the gain factor of 1000 does not vary with the amplitude of the input signal (up to 10 V).

The next stage in characterising this amplifier was to measure the bandwidth, in frequency, over which a signal is consistently amplified. This was performed by using a signal generator to output a white noise signal* of known amplitude. Similarly to the previous test this signal was then split with one output being passed directly to a digital oscilloscope and the being amplified before being passed to the oscilloscope. The digital oscilloscope was also used to process both of these signal by computing the Fast Fourier Transform (FFT) of both. When defining the frequency bandwidth of an electronic device it is usual to take the frequency that the voltage throughput has fallen to a factor of the square root of two times the maximum throughput. This is called the 3 dB bandwidth since:

$$20\log_{10}\left(\frac{1}{\sqrt{2}}\right) \approx -3 \text{ dB}. \quad (3.5)$$

More correctly the 3 dB bandwidth is defined as the frequency at which the power throughput has fallen by a factor of one half, i.e.:

$$10\log_{10}\left(\frac{1}{2}\right) \approx -3 \text{ dB}. \quad (3.6)$$

Figure 3.4 shows the result of the bandwidth measurement. It is clear from the figure that at frequencies below 10 kHz the output of the amplifier (green trace on upper plot) differed only from the generated noise (red trace on upper plot) by the gain factor of 1000. As the frequency increased the gain factor (blue trace on lower plot) ceased to be constant and started to decrease. Using Equation 3.5, the 3 dB bandwidth corresponds to the gain dropping to 731; this occurred at a frequency of 55 kHz, this is illustrated by the dashed line on the lower plot of Figure 3.4.

The final part of characterising the amplifier was to measure the input referred noise. As seen earlier in this section for the configuration of this amplifier (shown

*The **AG33220ADS** states that this device has a bandwidth, when generating noise, of 9 MHz.

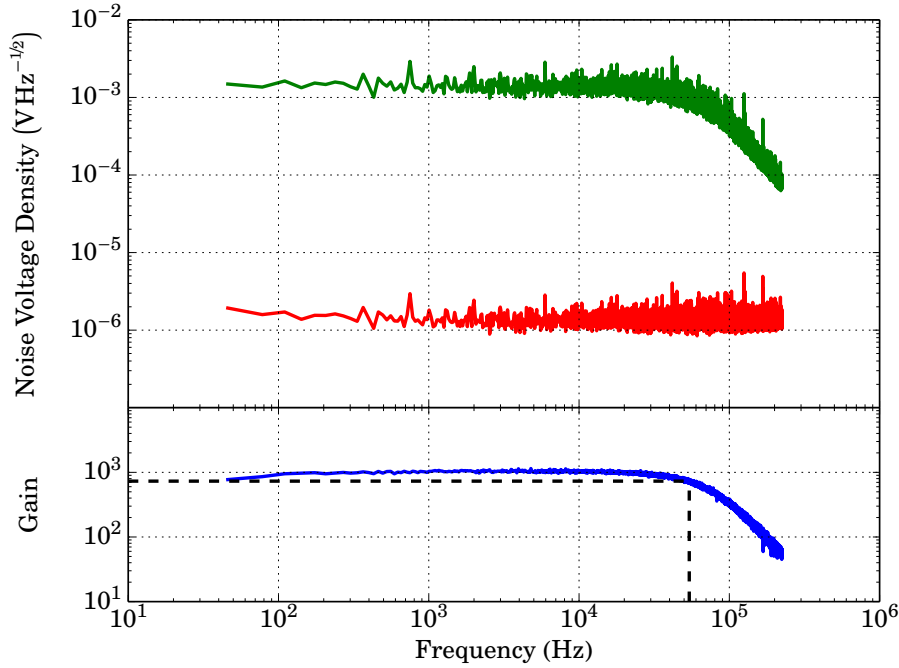


Figure 3.4: Bandwidth measurement of RTD amplifier. A white noise signal was generated by a signal generator, this was split with one feed being fed directly to the oscilloscope (red line) and one feed being amplified first (green line). The ratio (the gain of the amplifier) is shown on the lower plot the 3 dB level and corresponding frequency limit to the bandwidth are shown by the dashed line in the lower plot.

in Figure 3.1) the expected input referred noise was $10 \text{ nVHz}^{-1/2}$ (explained on Page 10). To measure this quantity the input of the amplifier was shorted and the output of the amplifier was measured as in the previous tests.

Figure 3.5 shows the measured noise spectrum for the amplifier (as referred to the input), measured up to 10 kHz. From this figure we can see that the internal noise is equivalent to a noise source of $10 \text{ nVHz}^{-1/2}$ at the input of the amplifier. This is the value which was predicted on Page 10 and this result, along with the results of the other tests carried out thus far, indicated that the amplifier system was performing as designed.

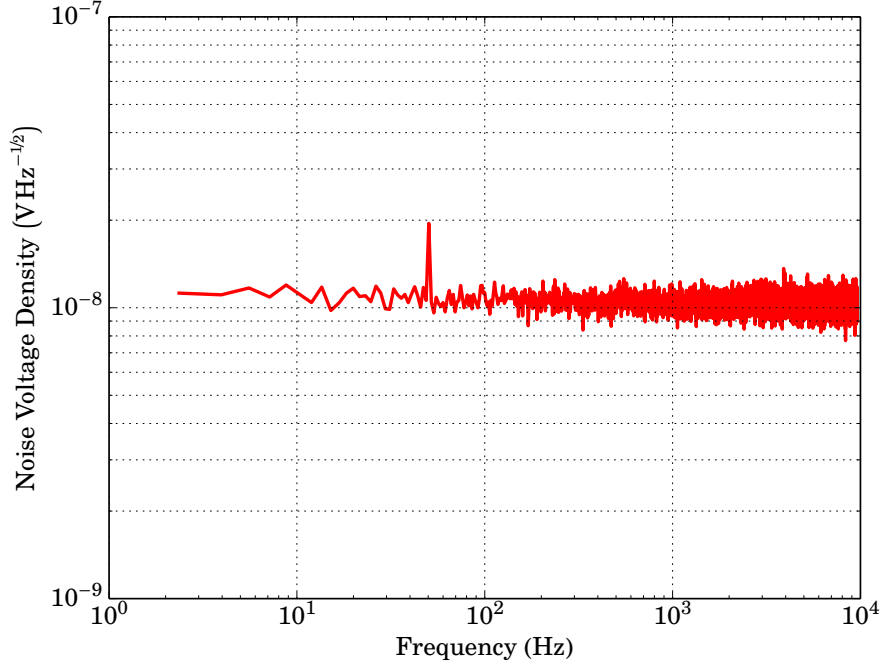


Figure 3.5: Measurement of the internal noise of the original amplifier, referred to the input of the amplifier. The measurement was performed by shorting the input of the amplifier and measuring the output of the amplifier with a digital oscilloscope, which also computed the FFT.

3.3.2 INITIAL BIAS SYSTEM

The amplifier only contributes one part to the total performance of the electronic system. The source of biasing current also plays a substantial role in the final performance. Unlike the amplifier the speed or bandwidth of this current source not of high importance since the IV measurements can be performed at a low frequency and noise measurements are measured with the device at a constant (DC) bias. The bias circuitry can however have a negative effect on measurement by either failing to provide a stable bias and thus causing some degree of *jitter* in a measurement or by adding an undesired level of noise (either as white noise or as finite tones). In the case of the current supply contributing additional noise, this could in-turn cause additional energy to be dissipated across the device being tested and thus affect the result.

In the first system used the current bias was provided by a Keithley 220 Programmable Current Source, this unit is capable of providing currents between 500 fA and 100 mA with a peak to peak noise level of between 400 ppm and 100 ppm depending on the output range specified*.

In order to test the effect of the current source two simple measurements were performed using a *dummy* device (typically a resistor with an appropriate value) as the DUT in Figure 3.1[†]. Firstly, a test was carried out to ensure that the output of the device was stable enough to allow for reliable measurements. This was performed in two parts: initially the Keithley 220 current source was set to a constant value (specifically 10 μ A) and the voltage across the *dummy* device (a 1 k Ω resistor) was measured multiple times using a reliable DAQ; after this the current across the resistor was increased in steps through a defined range and the voltage across the DUT was measured for each step. These tests were selected as they closely resemble the tests which were to be performed on the eventual SiCEB devices.

Figure 3.6 shows the measured jitter of a signal caused by the Keithley 200 unit. The signal varied around expected value of 10 mV by up to 550nV. The signal was measured by a trusted data acquisition system using shielded cables. This variation is equivalent to a peak-to-peak noise level of 110 ppm. The **Keithley220DS** states that when outputting a current of 10 μ A the expected peak-to-peak noise level is 100 ppm, although this is slightly lower than the measured value and thus indicates either an additional noise source or an issue with the unit, the measured jitter was still sufficiently low for preliminary measurements.

There are several possible reasons for the small amount of additional jitter measured in this test. Both the Keithley 220 unit used and the triaxial cables used as interconnects between the current source and the device under test were several years old and it is entirely possible that a number of small breaks were present in either the cable's inner guard layer or the insulator, this could cause current to be lost between the inner-most conductor and the outer-most shield layer and thus for current to be lost between these two. The age of the unit may also have meant that some of the internal components had degraded and were no longer working within their original specification. It is most likely that a combi-

*The full specifications of Keithley's 220 current source are stated in the **Keithley220DS**

[†]The 1 M Ω resistors shown in Figure 3.1 were used offer protection to sensitive detectors and were not included in this test.

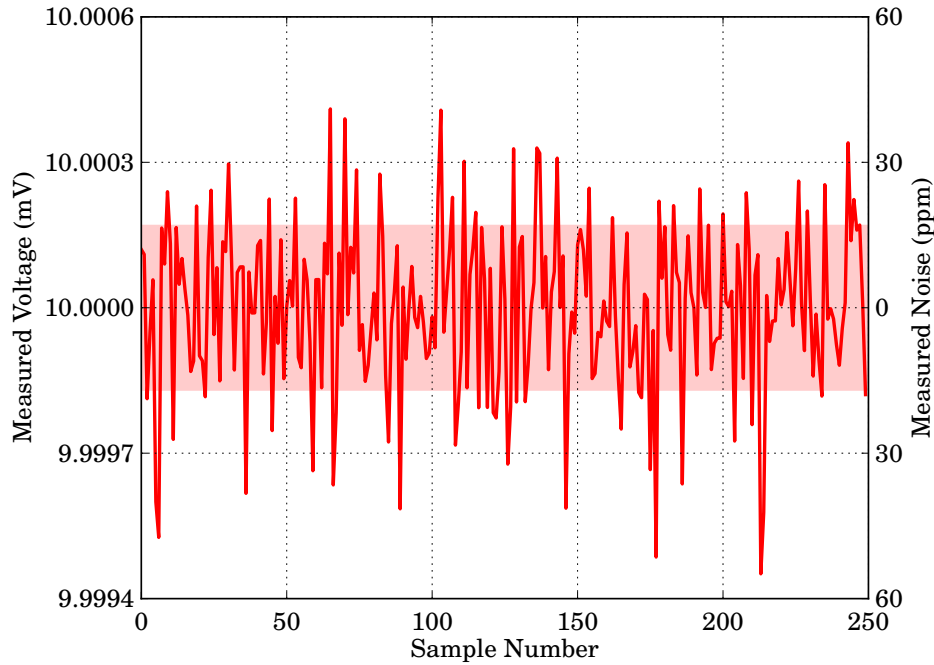


Figure 3.6: Jitter in a measurement caused by current supplied by a Keithley 220 Programmable Current Source. The current source was set to output a constant current of $10\ \mu\text{A}$ which was driven across a $10\ \text{k}\Omega$ resistor. Multiple measurements were made with a trusted data acquisition system. The primary vertical axis shows the voltage measured across the resistor in each measurement (the expected voltage was $10\ \text{mV}$); the secondary vertical axis shows the jitter or noise about the expected value in terms of noise parts per million; the shaded region shows the standard deviation of the noise about the expected value.

nation of these factors caused the additional noise measured. It is also possible that the degrading of the interconnecting cables could have made the system more susceptible to electromagnetic pickup.

The noise voltage spectrum measured across the resistor is shown in Figure 3.7, this did not resemble the *clean* spectrum seen in Figure 3.5, instead there was a substantial tone, due to mains pickup, seen at $50\ \text{Hz}$, along with several harmonics of this tone there were various other noise sources evident include two large clusters of tones at $4\ \&\ 8\ \text{kHz}$. This large clusters of noise tones were of

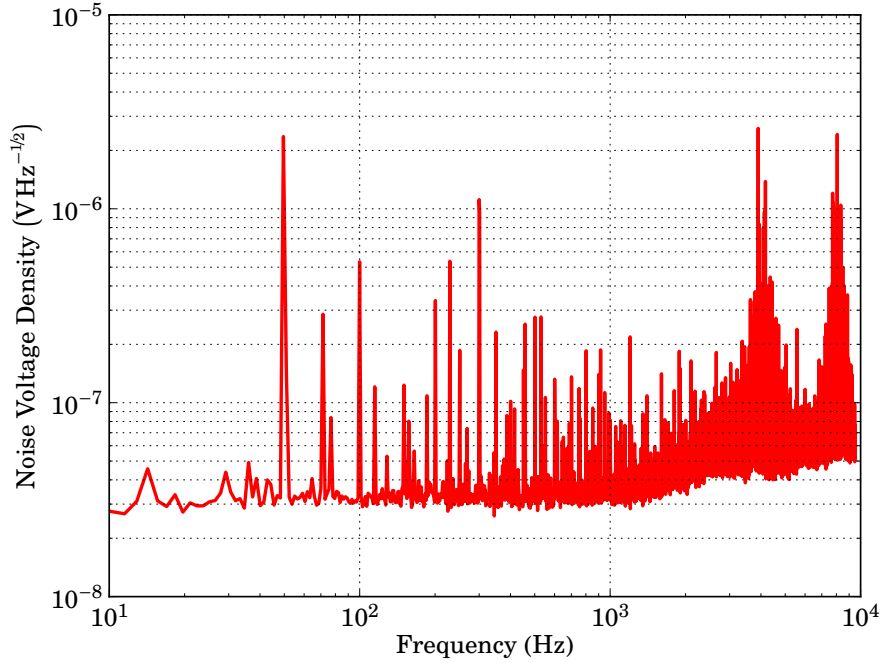


Figure 3.7: Noise spectrum measured across a resistor which was biased by the Keithley 220 Current Supply. A current of $10\ \mu\text{A}$ was driven across the resistor and the voltage (and noise spectrum) was measured using a digital oscilloscope. It was expected that noise spectrum would be dominated by the amplifier noise of $10\ \text{nVHz}^{-1/2}$, it is clear that this measurement shows a white noise level greater than this and is dominated by several other sources.

particular concern as they indicated that in addition to the desired DC biasing signal, there could have been a substantial amount of power dissipated in the device under test from these sources. The cause of this noise was confirmed by repeating the measurement across the resistor having disconnected the current supply. The result of this closely resembled that shown in Figure 3.5 and showed that the noise was due to the presence of the current supply. By disconnecting the interconnecting triaxial cable from the current supply, while leaving it attached to the device under test, it was found that the two clusters of high frequency tones were no longer present, this indicated that these were due to internal components within the current supply unit. However, many of the lower frequency tones remained,

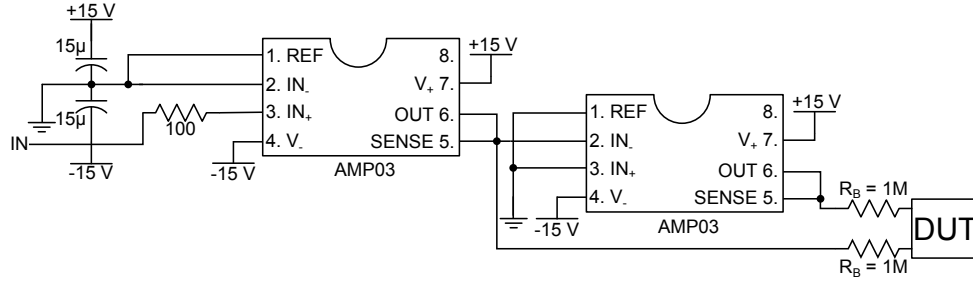


Figure 3.8: Circuit diagram for the custom made internal bias generator used with the first amplifier. A single ended input was fed to the non-inverting input of a unity gain amplifier, the output of this amplifier was split with one feed being supplied to the inverting input of a second unity gain amplifier. The output of this amplifier, along with that of the first, was then used to bias the device under test via a pair of biasing resistors.

these were attributed to electromagnetic pickup in the cable. This result meant that the Keithley 220 Current Supply would not be appropriate for use when carrying out noise measurement since there was sustainably contamination of the signal.

3.4 REVISIONS TO THE INITIAL BIAS SYSTEM

3.4.1 CHANGES MADE AND ADVANTAGES

As was found by the test described in the previous section, the Keithley 220 current source was not appropriate for noise measurement since there was substantial contamination (at AC frequencies) of the biasing signal from both electromagnetic pickup and the issues within the unit itself. To address this a simply circuit was constructed which generated a controlled differential signal, which had an amplitude determined by a controllable input signal. This signal could then be converted to a biasing current via a pair of resistors and the resulting current was found using Ohm's Law, measuring the voltage dropped across these biasing resistors.

There are several advantages to housing the biasing unit inside the casing of the amplifier, which during device testing was directly mounted to a cryostat. Firstly, since no interconnecting cabling was required, the possibility of electromagnetic pickup was greatly reduced. Secondly, due to the close physical proximity

of the amplifier and the current supply it was possible to have greater control over the grounding of these two components and thus remove any ground loops which could have offset a measurement or contributed to the total noise measured, further to this since the biasing signal was now sent using a differential connection there was no connection to ground across the device under test is fully isolated from any possible ground loops or other contamination from the ground line. Finally, since the amplitude of the current was not directly controlled by the bias generator but instead is governed by an external source, it was possible to produce a smooth range of currents, as opposed to Keithley unit which was only able to step current, all be it in relatively small steps.

The bias generator worked by using two unity gain amplifiers to generate a differential biasing signal, V_{in} , from a single-ended input. The input was fed into the non-inverting input of the first amplifier, the output of this was equal, in amplitude, to the input signal and was then split with one feed connected to the inverting input of the second amplifier. The output of the second amplifier was again equal in amplitude to the input signal but had the opposite sign, the output of this amplifier along with that of first amplifier served as the biasing voltage. This biasing voltage, V_{bias} , formed a differential signal and was given by:

$$V_{bias} = V_+ - V_-, \quad (3.7)$$

where V_+ and V_- are the outputs of the first and second amplifiers respectively. Since, in this case, the outputs of these amplifiers were $V_+ = +V_{in}$ and $V_- = -V_{in}$, the final biasing voltage was given by:

$$V_{bias} = 2V_{in}. \quad (3.8)$$

The biasing current, I_{bias} , across the device under test is the same as the current through the two biasing resistors, which from Ohm's Law is given by:

$$I_{bias} = \frac{V_R}{2R_{bias}}, \quad (3.9)$$

where V_R is the voltage dropped across the two biasing resistors. By measuring the voltage across the device under test, V_{DUT} , and from knowing the voltage generated by the bias circuitry, the voltage dropped across the biasing resistor was given by:

$$V_R = V_{bias} - V_{DUT}. \quad (3.10)$$

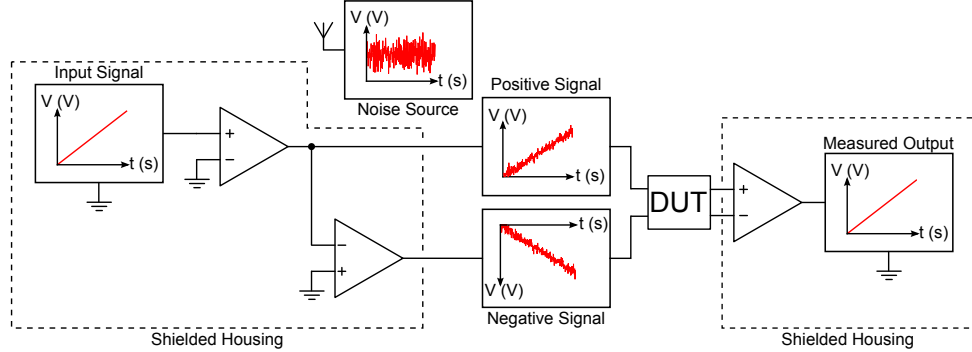


Figure 3.9: Rejection of common-mode noise in a differential signal bias and readout system. The two amplifiers which make up the differential signal generator produce two signals which are equal and opposite to each other and related in magnitude to the input signal. This is then carried, by a pair of wires, through an unshielded environment. Any electromagnetic pickup adds to both of these signals as a common-mode, this does not affect the difference, in amplitude, between the two signals and thus is not measured by the final differential amplifier.

By using the result of Equation 3.8 the above can be written as:

$$V_R = 2V_{in} - V_{DUT}. \quad (3.11)$$

Finally combining this with Equation 3.9, the biasing current can be calculated by:

$$I_{bias} = \frac{2V_{in} - V_{DUT}}{2R_{bias}}. \quad (3.12)$$

There were further advantages of this biasing regime, offered by the fact that the system now used a differential signal to bias the device under test. Since the device under test was now isolated from the ground line, which is often a source of signal contamination. This regime also offers a dramatic reduction in the effect of electromagnetic pickup. Since this differential bias generator produced two signals of equal and opposite voltage and since noise due to electromagnetic pickup would have added to both, this meant that the difference between the two signals, at any given time, remained the same and the output of the final amplifier, which only depended on this difference, was not affected. In terms of differential signals a change which maintains the same difference between the two signals is

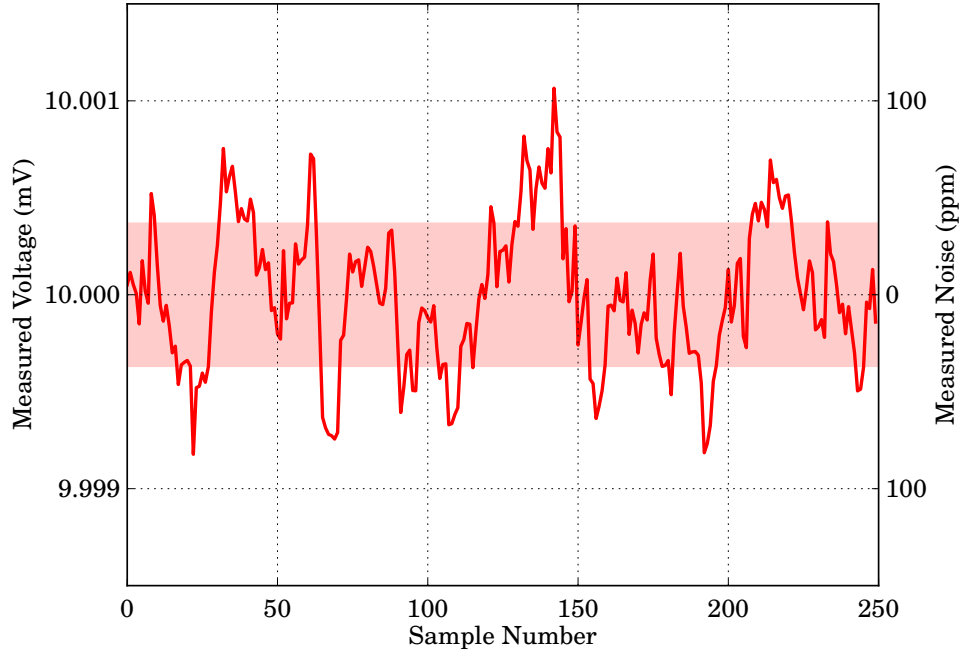


Figure 3.10: Jitter measured from custom made current bias generator. The input voltage to the system was set such that a current of $10\ \mu\text{A}$ flowed through the $1\ \text{k}\Omega$ resistor (which took the place of the device under test). The voltage across the resistor was measured using a trusted data acquisition system. The primary vertical axis shows this voltage (which was expected to be $10\ \text{mV}$); the secondary vertical axis shows the jitter or noise about the expected value, in terms of noise parts per million; the shaded region shows the standard deviation of the noise about the expected value.

referred to as a common-mode, when the difference between the two is affected there is said to be a normal-mode. This concept is illustrated in Figure 3.9.

3.4.2 PERFORMANCE OF UPDATED BIAS SYSTEM

In order to ascertain whether or not this current generator offered improved performance over the Keithley 220 the same test, which were described in Section 3.3.2, were repeated with the new system. Of particular interest were the results of measuring the noise spectrum produced by this system.

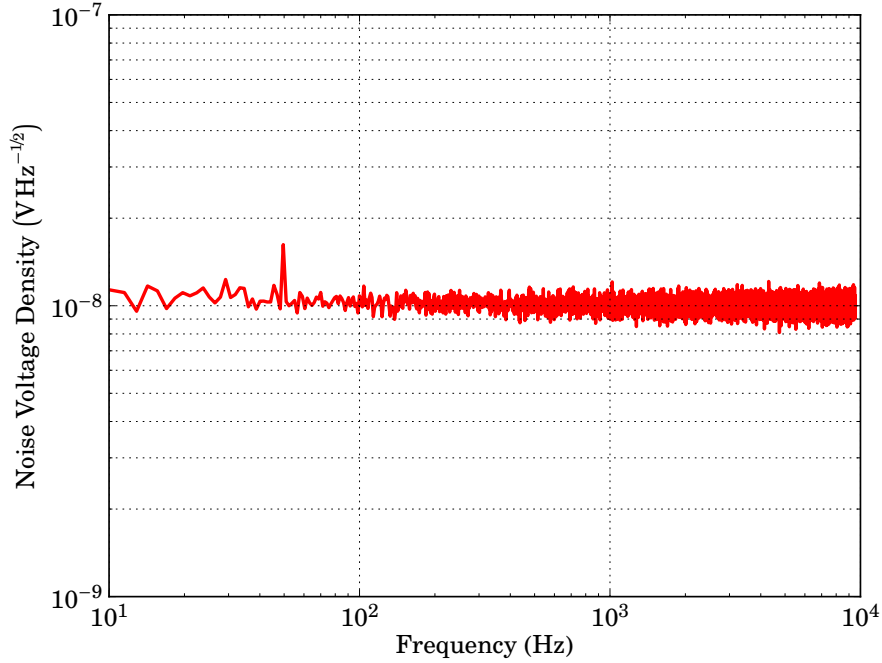


Figure 3.11: The noise spectrum measured across a 1 k Ω resistor biased using the custom made bias generator. When compared to the spectrum measured using the Keithley 220, shown in Figure 3.7, it is clear that the newer system showed very little contamination of this signal.

Figure 3.10 shows the jitter measured for current generator which replaced the Keithley unit. The measured peak-to-peak jitter for this system was 200 ppm which corresponded to a maximum variation of 1 μ V from the expected value. While this value is approximately twice what was measured in Section 3.3.2 for the Keithley unit (illustrated in Figure 3.6), the level was still deemed to be acceptable for IV characterisation.

The noise spectrum measured across a resistor, biased using the newer current generator, is shown in Figure 3.11. When compared to the corresponding measurement in Section 3.3.1 for the Keithley 220 (Figure 3.7) it is noted that the noise spectrum measured here is much cleaner; there are far fewer noise tones present and the two clusters of tones seen at higher frequencies in Figure 3.7 are no longer present, in fact the only undesired feature present within the spectrum

is noise tone at 50 Hz, this was due to the 50 Hz variation of the mains power. The white noise level measured in this test was $10 \text{ nVHz}^{-1/2}$ compared to a minimum value of $30 \text{ nVHz}^{-1/2}$ (rising to over $70 \text{ nVHz}^{-1/2}$) for the Keithley unit. In fact when the noise spectrum shown in Figure 3.11 is compared to the measurement made with the input of the amplifier shorted (Figure 3.7) it is clear that the two compare extremely favourably. This showed that this measurement was limited by the internal noise generated by the readout amplifier (as shown in Section 3.3.1).

From these tests it was clear that the revised biasing system offered a notable overall improvement when compared to the Keithley 220, despite there being a decrease in the stability of the bias signal produced, the improvements to noise spectrum, and the resulting reduction in unwanted power dissipated across the device under test, meant that this system was used for the preliminary testing of CEB devices.

3.5 FINAL TESTING SYSTEM

3.5.1 REASON FOR REPLACEMENT

Despite having reached a stage where the initial readout system was performing as well as could have been expected of it, it became clear, as testing of devices progressed, that its limitations were prohibiting the full characterisation of devices. When compared to list of desirable features for the readout system (as defined in Section 3.2) neither the second nor third points were met. That is to say that measurements of noise spectra were limited by the amplifiers own internal noise and that the amplifier did not offer sufficient bandwidth to allow the speed of response of a detector to be measured.

For these reasons it was decided to replace the initial readout amplifier and bias generator, which had been constructed from non-optimised components and designs already existing within the Department, with a new specifically designed system. This system would continue to offer a bias generator similar to the one described in Section 3.4.1 but with the added feature of being able to internally generate the voltage input to the bias generate, this feature was desired to offer an ultra-low noise DC bias, all be it at the slight cost of functionality.*

*Since this ultra-low noise level was only required when measuring noise spectra, the system could still be used in a way similar to the method described in Section 3.4.1 without any loss of

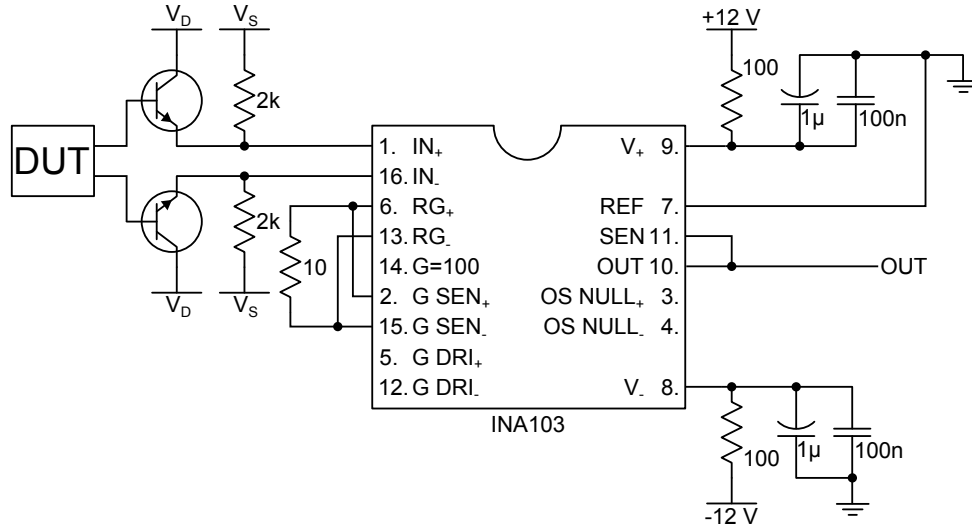


Figure 3.12: Final amplifier used for measuring voltage across devices. As opposed to the previous system (Figure 3.1) only one amplifier stage was used, the Texas Instruments INA103 amplifier, which was configured to offer a gain 600. In addition to the amplifier a matched pair of JFETs were used as a source follower. This improved coupling to the amplifier by offering a low output impedance. It also isolated the amplifier from the device being measured, thus resulting in a lower noise level.

3.5.2 FINAL READOUT SYSTEM

Figure 3.12 shows the amplifier used for the final stages of testing Silicon Cold Electron Bolometers. The main amplification was performed by a INA103 chip manufactured by Texas Instruments. However, in order to provide a low-impedance input to the amplifier, as well as isolating the device under test from the amplifier circuitry, a matched pair of junction field effect transistors (JFETs) were used to create a differential source follower to act as the input of the amplifier.

One disadvantage of this configuration was that the addition of the JFET source followers was that a offset voltage was added to the input of the amplifier. As explained by **HorowitzHill1989** this is the result of inconsistencies in the current produced by a given voltage across the gate and source of the JFET. The reason for these inconsistencies is due to this parameter being poorly controlled in the manufacture of JFETs. This could have been addressed by including functionality.

a second JFET, matched to the existing JFET, that acted to vary the source voltage to the first JFET such that there would have been no voltage offset at the output (which would have been at the drain terminal of this second JFET). This modification was not however applied since the differential input to the amplifier already necessitated the two JFETs be matched and the increase to quad-matched JFETs was prohibitively expensive for a non-critical improvement.

The preliminary testing had indicated that the previous amplifier's gain of 1000 was possibly excessive. To this end it was decided that a lower gain, of approximately 600, would be used in this case. The **INA103DS** does not provide a table of the required resistance across the gain setting pins to achieve this value, there is however the equation for the gain, G :

$$G = 1 + \frac{6000}{R_G}, \quad (3.13)$$

where R_G is the value of the gain setting resistor required to achieve a gain of G . Thus the value of the resistor required for a gain of 600 could be found as:

$$R_{G=600} = \frac{6000}{600 - 1}, \quad (3.14)$$

$$R_{G=600} \approx 10. \quad (3.15)$$

As had been performed for the previous amplifier (Section 3.3.1), a sinusoidal signal was split with one feed supplied to the input of the amplifier and the other, along with the output of the amplifier, measured using a digital oscilloscope. The gain of the amplifier could then be calculated by simply taking the ratio of these two. The results of this measurement are shown in Figure 3.13 where it can be seen that, for an input signal with an amplitude of 7.5 mV, there is uniform amplification at all amplitudes and the gain factor was 600.

The addition of the JFET source followers caused a further complication with this amplifier. Figure 3.14 show what happened when the amplitude of the input signal to the amplifier was increased above the 7.5 mV illustrated in Figure 3.13. In Figure 3.14 it is clear that there is a lower limit to the output voltage (green line shown on the secondary vertical axis) of approximately -4.5 V. In order to understand the origin of this limit and any significance it might of had on testing it is important, as always, to fully understand how these data were collected. As has already been mentioned the presence of the JFET source followers resulted

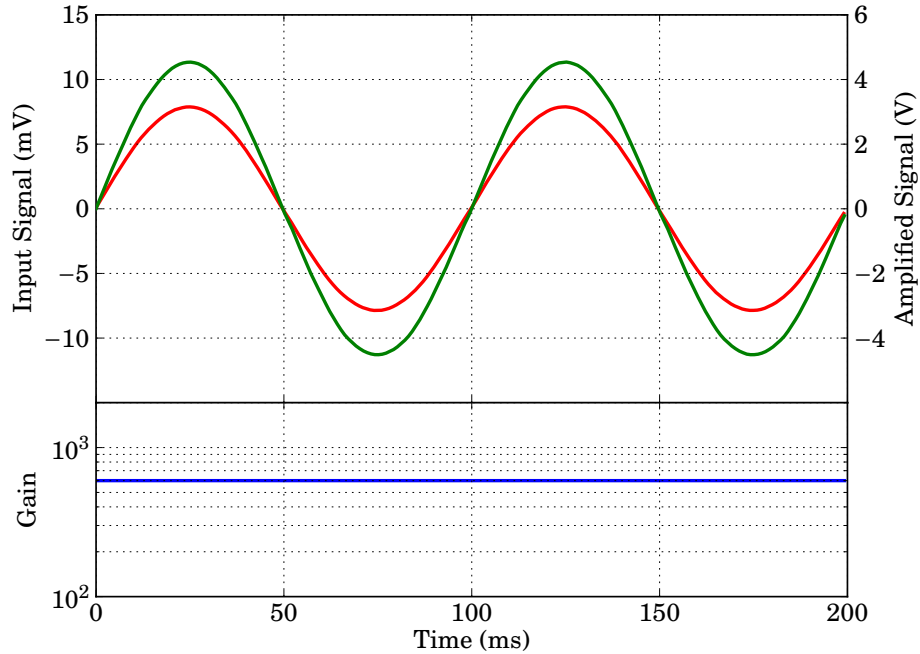


Figure 3.13: Gain measurement for the amplifier used in the final test of Silicon Cold Electron Bolometers. As in Section 3.3.1, a 10 Hz sinusoidal signal was supplied to the input of the amplifier and the output measured. Upper plot – Input signal (red, primary vertical axis) compared to the output of the amplifier (green, secondary vertical axis). Lower plot – Gain measured from the ratio of the output and input signals.

in an (undesired) DC voltage offset to the input of the INA103 amplifier. When measured this offset was found to be -6.59 V at the output of the amplifier (or -11 mV at the input), in order to simply correct for this in the measurement, the input of the digital oscilloscope (which was used for all the measurements in this section) was set to AC-coupling *****TO DO: ...maybe add glossary for this*****. This meant that values which were recorded as 0 V in the AC-coupled measurement corresponded to an output voltage of -6.59 V from the amplifier. The **INA103DS** explains that the amplifier is capable of a maximum voltage output range of ± 11 V. By dividing by the gain of the amplifier (600 in the configuration used) it was possible to calculate the range of input voltages, to the amplifier, for

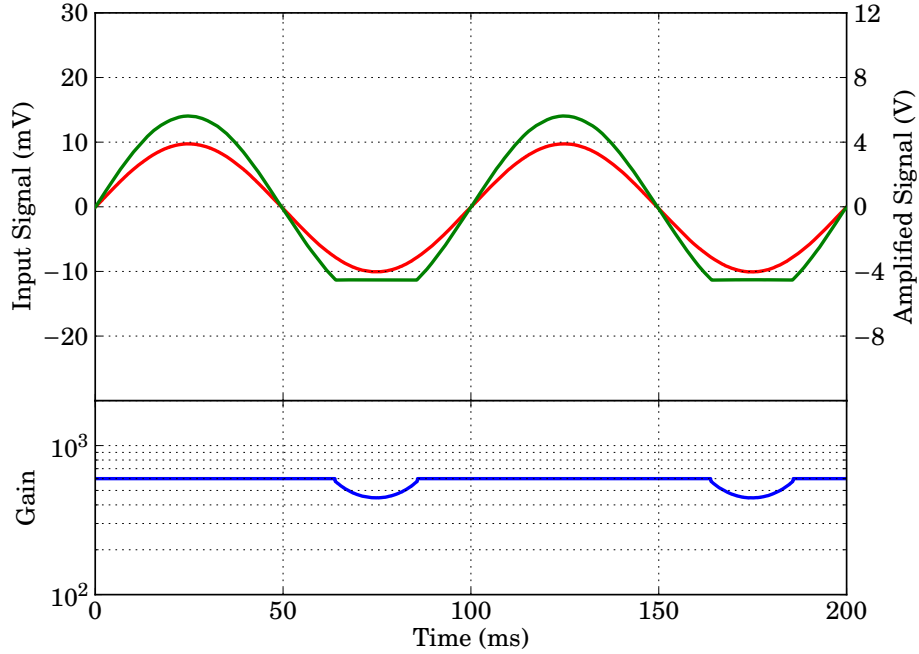


Figure 3.14: When the input to the final amplifier was increase above an amplitude of 7.5 mV an asymmetric response was noted. While positive signal continued to be amplified, by a gain factor of 600, the negative signal with the same magnitude became limited to a certain minimum value. Upper plot – Input signal (red, primary vertical axis) compared to the output of the amplifier (greed, secondary vertical axis). Lower plot – Gain measured from the ratio of the output and input signals.

which a correctly amplified output was attainable (i.e. those which corresponded to an output of less than ± 11 V); this was found to be ± 18.3 mV. As explained earlier however the JFET source follower used resulted in an offset voltage of -11 mV at the input of amplifier. When this was subtracted from the input range of the amplifier the effective range of input voltages, $V_{input_{eff}}$, was found to be

$$V_{input_{eff}} = V_{input} - V_{offset}, \quad (3.16)$$

$$= \pm 18.3 \text{ mV} - -11.0 \text{ mV}, \quad (3.17)$$

$$= \begin{matrix} +29.3 \\ -7.3 \end{matrix} \text{ mV}. \quad (3.18)$$

While this result has the advantage of meaning the amplifier system had an in-

creased range for positive signals, there was a severe restriction places on the amplifiers ability to handle negative signals. Fortunately the required measurable input voltage range for testing SiCEB devices was only of the order of ± 1 mV, with few circumstances existing where signals of greater magnitude were measured and none that would require measuring down to 7.3 mV across the device. For comparison the previous amplifier's input range, which did not suffer from any asymmetry, was ± 13 mV.

Since the restricted range of input voltage did not, in fact, affect the amplifier's suitability for the measurements being undertaking, despite this clearly being non-ideal, it was decided that there was no need to address this. As previously mentioned, the DC offset due to the JFET could have been removed via the addition of a second JFET on each input.

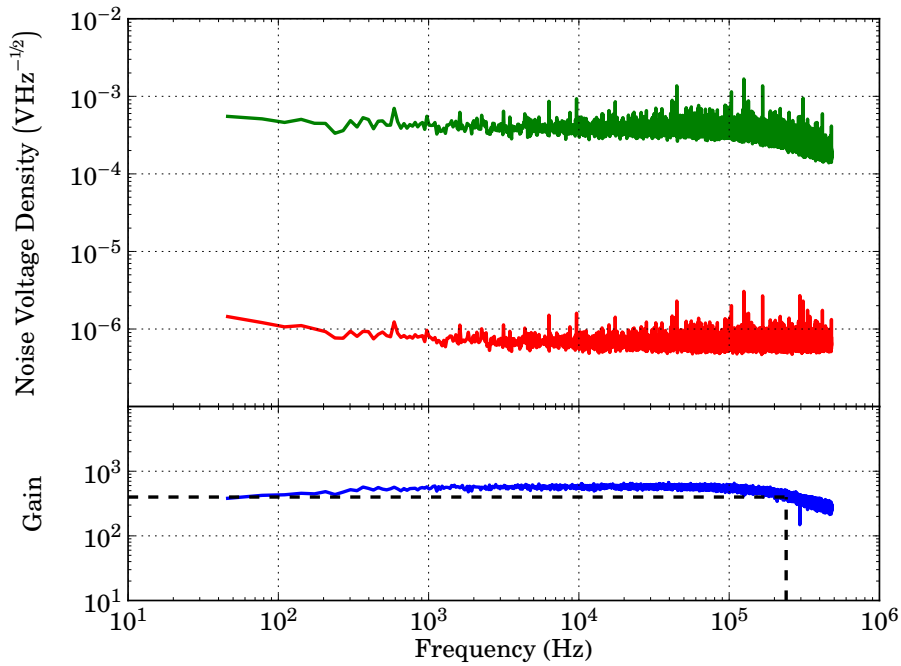


Figure 3.15: Bandwidth measurement of final amplifier. A white noise signal (red trace) was generated and supplied to the amplifier whose output (green trace) was also monitored. The ratio of these two (the gain, blue trace) was also calculated.

In order to measure the 3 dB bandwidth of this amplifier that same procedure was used as for the initial amplifier (described fully in Section 3.3.1), a signal generator was used to create a white noise signal which was input into the amplifier. The output of the amplifier, along with the output of the signal generator, were monitored using a digital oscilloscope. To measure the bandwidth of the amplifier the ratio of the input of the amplifier to its output (its gain) was measured, the results of this are shown in Figure 3.15. As explained by Equation 3.5 the edge of the 3 dB bandwidth corresponds to the frequency at which the gain has fallen by a factor of $\sqrt{2}$. The lower plot in Figure 3.15 shows the measured gain with the dashed lines illustrating the 3 dB level, which was a gain of 424, and the corresponding frequency found to be 240 kHz. This shows the amplifier offered a substantial improvement compared to its predecessor whose 3 dB bandwidth was equal to 55 kHz (calculated on page 12). Although the **INA103DS** does not provide a figure for the expected bandwidth of the amplifier when operating with a gain of 600, it does provide values of 6 MHz and 800 kHz for gains of 1 and 100 respectively, this seems to indicate that the value of 240 kHz, at a gain of 600, is to be expected.

Figure 3.16 shows the measurement of the internal noise of the final amplifier. This was measured with the input to the amplifier (the gates of the two JFET source followers) shorted such that there was a differential signal of 0 V at the input of amplifier. The output of the amplifier was fed to a digital oscilloscope, which computed the Fourier Transform of the signal. This was then divided by the gain (measured in Figure 3.13) to give the input referred internal noise of the amplifier. From Figure 3.16 it can be seen that the white noise level of this noise spectrum is approximately $1.5 \text{ nVHz}^{-1/2}$ and the spectrum is white from a few hundred hertz up until the end of the measurement at 10 kHz.

When compared to the corresponding measurement for the previous amplifier, shown in Figure 3.5, two key differences are immediately apparent. Firstly, the newer amplifier has a substantially lower noise level, with the white noise floor of the previous amplifier having been $10 \text{ nVHz}^{-1/2}$ compared to the newer device's level of $850 \text{ pVHz}^{-1/2}$; this notable improvement was the key reason for switching to the newer amplifier. Secondly, there is a more pronounced level of $1/f$ noise visible in the spectrum for the newer amplifier compared to its predecessor, while indeed undesirable the **INA103DS** indicates that this is to be expected for this device and

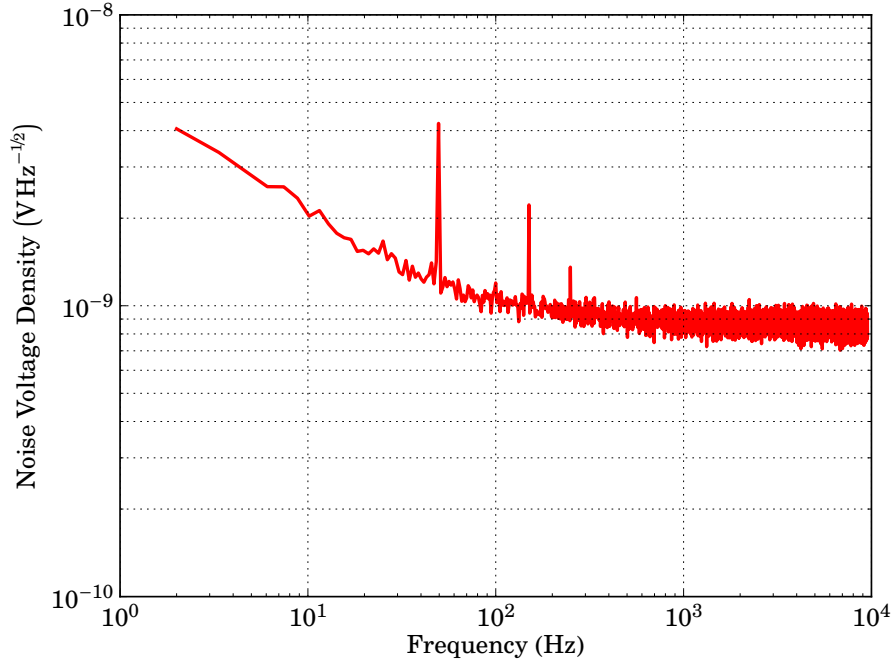


Figure 3.16: Measurement of the internal noise, referred to the input, for the final amplifier. Measured for a shorted input of the amplifier.

it is worth noting even when allowing for this additional noise the newer amplifier still offered low noise at these frequencies than the previous amplifier.

These two tests showed that the replacement amplifier offered a notable improvement, in all areas, over the initial amplifier used and also showed that despite the newer device having some limitations not present in its predecessor (principally the asymmetric limit to the input voltage, shown in Figure 3.14), these limitations did not stop it from being fit for the testing required.

3.5.3 FINAL BIAS SYSTEM

For simplicity of integration a biasing system, similar to that described in Section 3.4, was integrated into this final system. The circuitry for this, shown in Figure 3.17. The only difference in operation between this circuit and the system used previously was the relation between the input signal and the differential

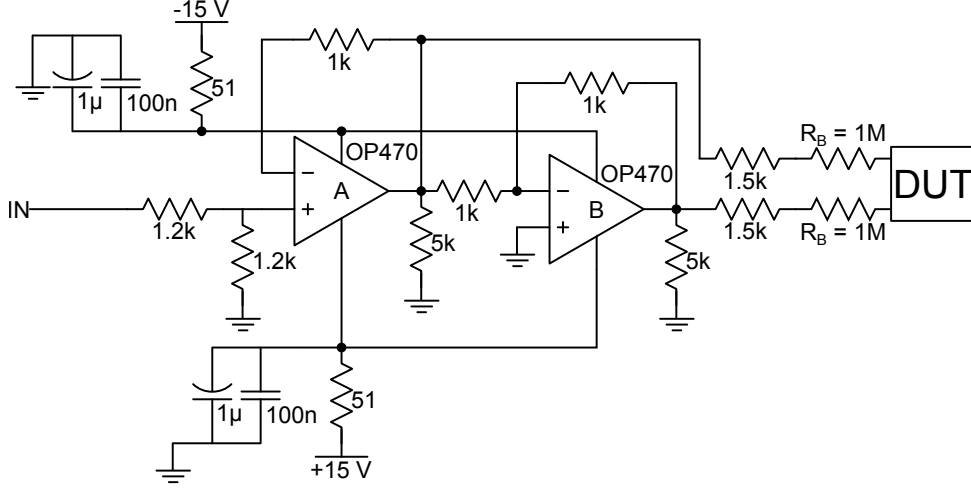


Figure 3.17: Circuitry used to generate a differential signal used to bias the device under test. The principle is the same as described in Section 3.4.

output. For the previous system this was 1 : 2, meaning for an input of 1 V a differential signal of 2 V was output (as explained on Page page 19). The key difference here was that although both of the OP470 amplifiers (manufactured by Analog Devices and in fact housed within a single package) were configured to provide a gain factor of unity, an additional potential divider was included at the input of the first amplifier. This divider (the two 1.2 k Ω resistors seen in Figure 3.17) acted to reduce the input of the first amplifier by a factor of a half. This meant that the output of each of the amplifiers was equal to one half of the input voltage, thus the total differential voltage at the output was the same as the input voltage. As in the previous case the device was biased via a pair of 1 M Ω biasing resistors and the biasing current can be calculated similarly to the method on page 19. For this system, using Equation 3.7 the biasing voltage V_{bias} was simply given by:

$$V_{bias} = V_{in}, \quad (3.19)$$

where V_{in} was the input voltage to the bias generator. This meant that the biasing current, I_{bias} , across the device under test was calculated as:

$$I_{bias} = \frac{V_R}{2R_{bias}} \quad (3.9 \text{ revisited})$$

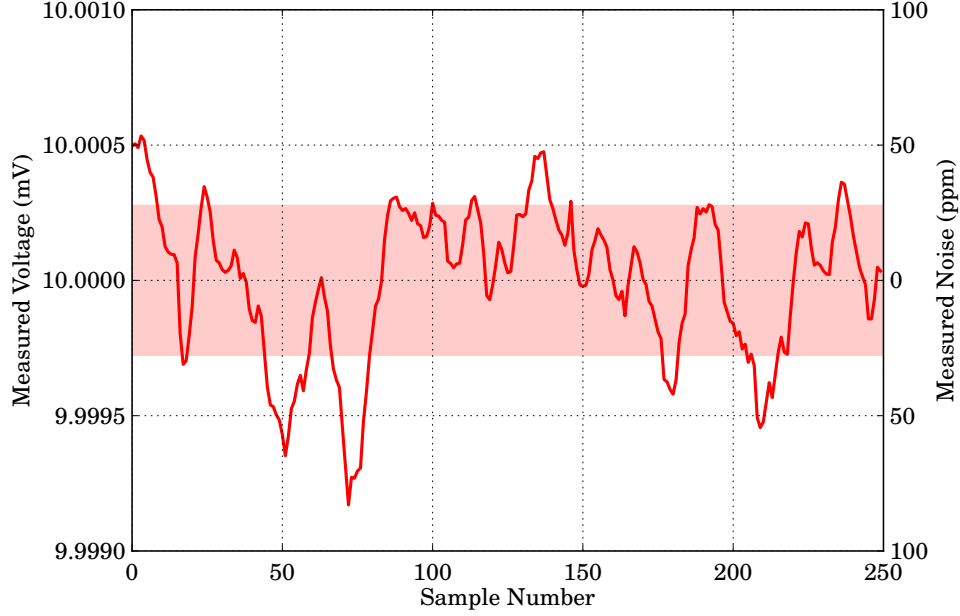


Figure 3.18: Measurement of jitter from the bias generator used with the final readout amplifier. The generator was configured to produce a biasing current of $1 \mu\text{A}$ which was driven across a $10 \text{ k}\Omega$ resistor.

where V_R is again the voltage dropped across the biasing resistors and, given the result shown in Equation 3.19, was calculated by:

$$V_R = V_{in} - V_{DUT}, \quad (3.20)$$

where V_{DUT} is the voltage measured across the device under test. Finally combining this with Equation 3.9 gave the final relation for the biasing current:

$$R_{bias} = \frac{V_{in} - V_{DUT}}{2R_{bias}}. \quad (3.21)$$

As for the previous biasing systems it was important to measure the jitter in the current produced. This was performed by configuring* the bias generator to produce a current of $1 \mu\text{A}$ which was driven across a $10 \text{ k}\Omega$. This meant that

*The input voltage to the bias generator for this measurement was provided by using the systems on board voltage (controlled through a potential divider) rather than an external source.

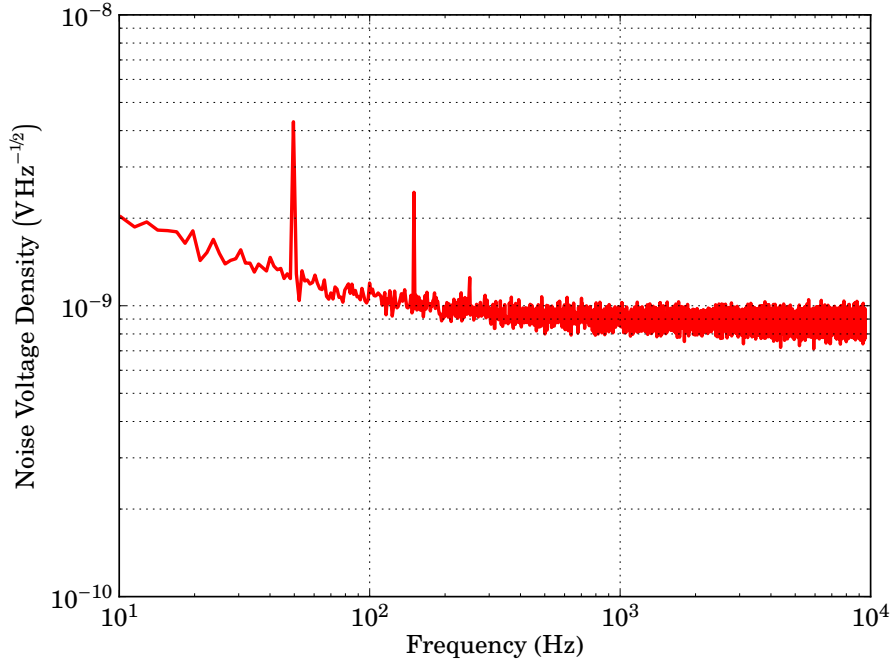


Figure 3.19: Noise measurement for bias generator used in conjuncture with final readout system. A low value resistor ($\approx 10 \Omega$) was placed across the output generator and the amplifier was used to amplify the signal. The output of the amplifier was read by a digital oscilloscope which computed the noise spectrum.

the expected voltage measured across the resistor, according to Ohm's Law, was 10 mV. Figure 3.18 shows the results of this measurement. The maximum variation from the expected value was 800 nV which corresponded to a peak-to-peak jitter of 160 ppm. While this was still not as low as the jitter measured for the Keithley 220 unit, which was 110 ppm, it was in fact an improvement of the value of 200 ppm which was measured for the previous bias generator in Section 3.4.2. Since the jitter of the previous system had caused no problems, there was no reason to conclude that any issue would be presented here.

Figure 3.19 shows the noise spectrum, measured using the amplifier described in Section 3.5.2, for a device (a low resistance resistor) biased by the system shown in Figure 3.17. Comparison between this figure and the noise spectrum shown in

Figure 3.16 shows that the dominating noise is from the internal processes in the amplifier and the bias generator did not contribute any additional noise to this measurement. This is that same as had been found for the previous bias generator system and is not a surprise considering the similarities, in operational principle, between the two systems.

3.6 CROSS-CORRELATED NOISE MEASUREMENT

Despite the improved (lower) noise limit of the system detailed in Section 3.5 this system was, at best, only able to measure noise generated within a device at optimum bias*. To allow a full study of the sensitivity of a device it was important to be able to measure the noise in the device over the greatest possible range of biases. To this end an innovative solution was devised to reduce the noise level of the readout system. This was to split the voltage readout of the device between two identical amplifiers and then to use a computer to cross-correlate *****TO DO: Add glossary entry***** the output of these to effectively remove the noise contribution of the amplification.

3.6.1 CONVOLUTION & CROSS-CORRELATION

The convolution of two signal or functions is a third function whose amplitude is given by the area overlap of the f and g when one of the functions is reversed and then translated across the other function. Common applications of convolution include: measuring the response function to an impulse function (**Callier1978**), in probability the convolution of two independent variables gives the probability distribution (**Hogg2012**), in acoustics and sound-engineering reverberation is the convolution of an original signal with reflections (echos) from surfaces (**Begault2007**), in signal processing a weighted average of a signal is a convolution.

In time-space the convolution of two functions, f and g , is written as $f * g$. Mathematically this is computed by reversing one of these functions such that $f(t) \rightarrow f(t - \tau)$ and then translated across the other function. This can be written

*The dependance of various noise sources to the bias, or more correctly the bias dependant responsivity, is explained on Page ## in Chapter ##. *****TO DO: Update this.*****

as an integral as,

$$(f * g)(t) \stackrel{\text{def}}{=} \int_{-\infty}^{\infty} f(\tau) g(t - \tau) . \quad (3.22)$$

Convolution is commutative so $f * g = g * f$ or more completely:

$$\begin{aligned} (f * g)(t) &\stackrel{\text{def}}{=} \int_{-\infty}^{\infty} f(\tau) g(t - \tau) \\ &= \int_{-\infty}^{\infty} f(t - \tau) g(\tau) . \end{aligned} \quad (3.23)$$

It is, perhaps, easiest to understand convolution in the time-domain graphically. This is shown in Figure 3.20. From this figure it can be seen that the value of convolution at any time τ is given by the area overlap of the two function (shown as the highlighted regions in Figures 3.20d to 3.20h) when the leading non-zero value of the reversed function ($g(t)$ in this case) is at τ .

Convolution can be thought of much more simply in the frequency domain. As explained by **Bracewell2000** Convolution Theory states that the Fourier Transform of the convolution of two functions is the multiplication of the Fourier Transforms of the functions. This can be written as:

$$\mathcal{F}(f * g) = \mathcal{F}(f) \times \mathcal{F}(g) \quad (3.24)$$

where \mathcal{F} is the Fourier Transform and f and g are functions.

*****TO DO: For any acronyms which have glossary entries, make the glossary the main key used and include first = { gls acr:*****

*****TO DO: Finish this chapter with a nice table showing the relative performance of the four systems used: RTD+Keithley, RTD+Current Gen, Final Amp, Cross correlated*****

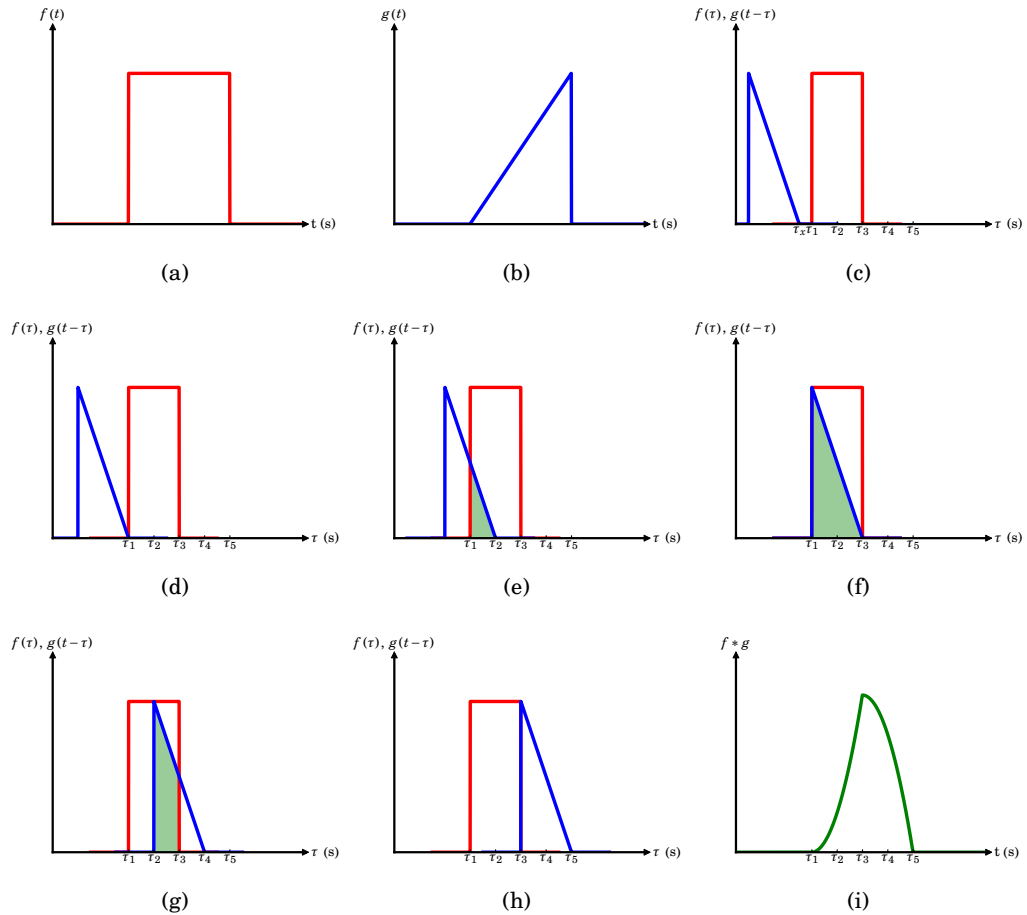


Figure 3.20: Graphical representation of convolution in the time domain. Two function $f(t)$ and $g(t)$, shown in parts (a) and (b) respectively. To find the convolution of the two functions one function is reversed in time (in this case $g(t)$ was chosen), this is shown in part (c), and then translated across the other function, shown in parts (d) through to (h). The value of the convolution at any time, τ , is the area overlap (shown as the highlighted areas in parts (d) through to (h)) of the two functions when the leading non-zero value of the translated function is at τ . The convolution function is shown in part (i).

Acronyms

CEB Cold Electron Bolometer. 7, 8, *Glossary*: Cold Electron Bolometer

DAQ Data acquisition unit. 9, 15

FFT Fast Fourier Transform. 12, 14, *Glossary*: Fast Fourier Transform

IV current-voltage measurement where one of the quantities is varied and the response in the other is recorded. 8, 9, 14, 22

JFET Junction Field Effect Transistor. 24, *Glossary*: JFET

RTD Resistance Temperature Detector. 8, *Glossary*: Resistance Temperature Detector

SiCEB Silicon Cold Electron Bolometer. 7, 15, *Glossary*: Silicon Cold Electron Bolometer

SQUID Superconducting QUantum Interference Device. 7, *Glossary*: SQUID

Glossary

Silicon Cold Electron Bolometer A form of Cold Electron Bolometer where the central absorbing island is made from silicon and the tunnelling contacts are Schottky barriers formed naturally between the silicon and the superconducting contacts. 7

3 dB bandwidth The frequency at which the throughput of an electrical circuit or component has fallen by a factor of 3 dB (one half in power or root two in amplitude). 12, 29

Cold Electron Bolometer A bolometric detector that utilises tunnelling contacts as both sensitive thermometers as well as to offer direct electron cooling. The main study of this work. 7

Common-mode A signal which adds to both lines of a differential pair with the same sign and thus does not alter the voltage difference between the pair. This should be rejected by the measurement system. 20, 21, *See also:* differential signal & normal-mode

Differential signal A differential signal sends voltages across a pair of wire as opposed to a single conductor. The voltage is measured by an amplifier which measures the voltage difference between the two wires. Usually the two conductors have equal and opposite voltage. Only changes which alter the voltage difference between the two are measured. 19, 20, 29–31, *See also:* common-mode & normal-mode

Electromagnetic pickup Electromagnetic pickup describes the phenomenon of stray electronic signals coupling to another signal and degrading the signal

quality. This is often from signals on ground or power lines or from radio signals coupling to poorly shielded cabling. 16, 20

Fast Fourier Transform An algorithm used to compute the Fourier Transform of a signal. As is implied by the name a Fast Fourier Transform is notably faster than other methods. The most common method was constructed by **Cooley1965** and involves breaking down the matrix into smaller matrices and multiplication factors. 12, *See also:* Fourier Transform

Fourier Transform A transform function which converts a spatial signal into a one in the frequency domain or vice versa. 29

Ground loop An unwanted current which flows between two points which are suppose to be at the same potential. A ground loop is created when two circuits are independent except for sharing a common connection to ground, if this connection has a non-zero resistance and one of the circuits has an additional connection to ground, this and the common resistance to ground, act as a potential divider causing some voltage to be dropped across the resistor and thus a current to flow to ground. This current can then flow back through the circuit from other ground points. 18

JFET Junction Field Effect Transistor. A three terminal semi-conductor based electronic component. A potential applied to the middle of the three terminals (the gate) controls the size of a depletion region between the other two terminals (the source and the drain). They are commonly used as switches, amplifier or as a resistor whose resistance can be controlled via a voltage. 24, 25

Jitter The amount a supposedly constant signal varies about the expected value due to electronic noise or other influences. 15, 16, 21, 22, 32

Normal-mode A signal which adds to the two conductors of a differential pair with opposite signs, or to only one of the conductors, and thus alters the voltage difference between the pair. This is measured at the readout stage. 21, *See also:* common-mode & differential signal

Potential divider An electrical component used to reduce a voltage by a defined factor. Typically made of a pair of impedances one (Z_1) in line to the output and the other (after the first) to ground (Z_2). The voltage at the output is equal to the input voltage multiplied by the ratio of the impedance to ground to the total impedance. That is to say $V_{out} = \frac{Z_2}{Z_1+Z_2} \times V_{in}$. 31

Resistance Temperature Detector A secondary thermometer where the electrical resistance of the thermometer is usually inversely proportional to temperature. 8

Source follower An element of an electrical circuit which utilises a transistor (usually in the form of a JFET) as a voltage buffer. This is normally to offer a low input impedance to subsequent electronic components or to isolate components being measured via a high input impedance. 24, 25, *See also*: JFET

SQUID Superconducting QUantum Interference Device - a type of low-noise current amplifier, typical used at cryogenic temperatures. 7

Triaxial cable A form of electronic interconnect cable often used in sensitive low current measurements. It is similar the more standard coaxial cable but includes an additional inner-shield (guard) in an attempt to reduce any leakage current from the central conductor to the shield. 15

White noise Noise is being defined as being *white* if it is present at all frequencies and has a constant mean amplitude across these frequencies. 12, 14, 29

Appendices

Appendix A

Appendix title

... some text ...

List of Figures

3.1	Initial readout system using RTD amplifier and programmable current source	9
3.2	Noise model of series amplifiers	10
3.3	Gain measurement of original amplifier	11
3.4	Bandwidth measurement of original amplifier	13
3.5	Input referred noise of original amplifier	14
3.6	Jitter from a Keithley 220 Current Source	16
3.7	Noise spectrum from a Keithley 220 Current Source	17
3.8	Internal bias generator used with initial amplifier	18
3.9	Rejection of common-mode noise in a differential bias and readout system	20
3.10	Jitter from initial, custom made, current bias system.	21
3.11	Noise spectrum from original bias generator system, used in conjuncture with the initial amplifier.	22
3.12	Final voltage Readout Amplifier	24
3.13	Gain measurement of final amplifier	26
3.14	Asymmetric limit to input of the final amplifier	27
3.15	Bandwidth measurement of final amplifier	28
3.16	Measurement of the internal noise, referred to the input, for the final amplifier.	30
3.17	Differential bias generator used with final readout system.	31
3.18	Measurement of jitter from the bias generator used in conjuncture with the final readout system.	32
3.19	Noise measurement bias generator used in conjuncture with the final readout system.	33
3.20	Graphical representation of convolution in the time domain.	36

List of Tables

Index

text, 5

text is a useful thing for those who which to
 read it, 1

NUMBER OF REMINDERS: 5